Hindawi
Advances in Materials Science and Engineering
Volume 2021, Article ID 3027640, 10 pages
https://doi.org/10.1155/2021/3027640

Research Article

On Factors behind the Reasonable Failure Mode of Concrete-Filled Circular Steel Tubular Composite Frame

Yang-bing Liu,[1] **Ping-ping Cui**,[2] **and Fang Chen**[3]

[1]*College of Civil Engineering, Nanyang Institute of Technology, Nanyang 473004, China*
[2]*College of Intelligent Manufacturing, Nanyang Institute of Technology, Nanyang 473004, China*
[3]*College of Civil Engineering, Chongqing University, Chongqing 400045, China*

Correspondence should be addressed to Yang-bing Liu; liuyangbing@tsinghua.org.cn

Received 10 September 2021; Accepted 26 November 2021; Published 22 December 2021

Academic Editor: Luigi Di Sarno

As the most basic structure, the concrete-filled steel tubular (CFST) frame has been widely used in various structures and systems. Compared with conventional reinforced concrete structures and steel structures, CFST structures in strong earthquake showcase more complicated strength and deformation behavior because there are many factors underlying the failure mode. Furthermore, according to the specifications at home and abroad, the corresponding design method to achieve reasonable failure modes for CFST structures has not been clarified. Based on a destructive test on steel beam-CFST plane frames under constant axial load and lateral load, the fiber mode method and solid element model method are adopted to simulate the failure process of the test frames. Based on finite element model simulations and tests, the fiber model method is proposed to carry out the pushover analysis on the CFST frame structures. The factors behind the reasonable failure mode of steel beam-concrete-filled circular steel tubular (CFCST) frame structures are analyzed. Furthermore, the law and influencing factors behind the ratio of flexural capacity of column to beam, the ratio of line stiffness of beam to column, and the ratio of axial compression on the deformation, bearing capacity, and failure modes of the structure are discussed. Some suggestions on the design of reasonable failure mode of steel beam-concrete-filled circular steel tubular (CFCST) frame structures are proposed.

1. Introduction

The failure mode under the strong earthquake is one of the most important factors behind the seismic performance of the structure. Choosing a reasonable failure mode and making reasonable adaptation can help improve the seismic performance of the structure under large or even super large earthquakes and reach the performance goal of "no collapse under large earthquakes." As the most basic composite structure, the concrete-filled steel tubular (CFST) frame has been widely used in the CFST frame structure, CFST frame-core tube structure, and other structural systems. Compared with conventional reinforced concrete structures and steel structures, CFST structures in strong earthquake showcase more complicated strength and deformation behavior because there are many factors behind the failure mode. Furthermore, the corresponding design method of the reasonable failure modes for CFST structures has not been clarified in the building specifications at home and abroad. Therefore, it is necessary to further study whether the control measures of RC structure and steel structure for the reasonable failure mode of frame structure system in the existing specifications are suitable for the CFST frame.

Zuo et al. [1] analyzed the seismic performance of RC frames, which are designed according to Chinese seismic regulations and specifications, with different column-to-beam flexural strength ratios (CBFSRs) based on numerical simulations. The RC frames subject to near-field pulse-like and far-field nonpulse-like ground motions have been compared. CBFSRs were proposed for achieving the strong column-weak beam failure mode with an 80% guarantee rate for different seismic hazard levels and ground motion characteristics. Luo et al. [2] proposed an elaborate finite element modeling method for concrete-filled circular steel tubular composite space frame

and conducted pseudodynamic analysis on a two-story circular CFST column-composite beam space frame. Ye et al. [3] studied the weak beam-strong column design method of RC frame structures and proposed the method for designing strong column and weak beam. Wang et al. [4] and Wang and Han [5] carried out experimental study and simulation on the nonlinear finite element of the CFST frame structures and analyzed the parameters of the main factors for the mechanical properties of the CFST frames. Ding et al. [6] took the steel-concrete composite frame structure as the object to preliminarily explore the effects of various horizontal seismic wave conditions on the displacement, stress, axial compression ratio, and other time-history responses of the composite frame structure, as well as the distribution mechanism of plastic energy dissipation, the formation mode of plastic hinge, and failure mechanism of the frame. Liu et al. [7] used OpenSees software to analyze the finite parameters on seismic performance of CFST frames. Liu et al. [8] studied the failure mode of composite beam-CFST column frames and discussed how the ultimate moment ratio and beam-column line stiffness ratio affect the structural yielding mechanism.

Fang et al. [9] conducted an experimental study on concrete-filled and four bare steel EHS beam-column specimens under combined compression and cyclic bending, evaluated the existing design methods for predicting the moment resistance of the considered members, and proposed a preliminary design equation for ductility prediction. Fam et al. [10] evaluated the strength and ductility of CFST short columns and beam-column members under different bond and end loading conditions. Tao et al. [11] put forward the material models for simulating rectangular CFST stub and slender columns.

According to the specifications of different countries, when it comes to the failure mode of a strong column and weak beam in RC frame structure, every nation upholds the idea that the flexural capacity of the section, which forms the plastic hinge, remains unchanged, and the flexural capacity of the section in which plastic hinge is undesirable is increased in order to form plastic hinge only in the desirable position even under the input of ground motion of large earthquakes or even super earthquakes. Thus, the same idea can be used to realize the failure mode of strong column and weak beam in CFST frame structure, that is, to increase the ratio of the flexural bearing capacity of column end to that of beam end.

Based on the existing tests, the fiber modeling method and solid finite element method were, respectively, adopted to analyze and verify the elastoplastic model of the steel beam-concrete-filled circular steel tubular (CFCST) frames. A scientific and reasonable analysis model of the whole structure was established to compare the results of the analysis. Then, the pushover method was used to conduct the parametric analysis on the influencing factors of the failure mode of CFCST frame structures.

2. Elastoplastic Model

Two typical fiber models provided by Perform-3D [12] were used to define the beam section and column section. The axial force and nonlinear moment in-plane (the out-of-plane moment is elastic) have been taken into consideration in the fiber of beam section. The interactive behavior of axial force and moments in two directions can be considered in the fiber of the column section. Although the fiber model method can effectively simulate various components, the fiber model method is a simplified numerical analysis method and cannot accurately analyze the three-dimensional stress and the bond-slip between steel tube and concrete elements when it comes to the study on the mechanical properties of composite members. The solid finite element method can solve this problem well and verify the results of the fiber model method.

Elastoplastic analysis on the solid model was carried out based on ABAQUS software. The outer steel tubes and joint ring plates of steel beams and columns were modeled based on quadrilateral shell elements (S4). The inner concrete was modeled by a three-dimensional solid element (C3D8R). The interface contact between steel tube and concrete, the contact between steel beam, ring plate, and steel tube at joints, and the contact between stiffening plate and steel tube at column foot were also considered [13].

The stress-strain relation model of steel tube and steel plates was based on the contacts elastoplastic stress-strain relation model proposed by Han et al. [14]. Figure 1(a) indicates the stress-strain curve, where $f_e = 0.8f_y$, $\varepsilon_e = 0.8f_y/E_s$, $\varepsilon_y = 1.5\varepsilon_e$, $\varepsilon_h = 10\varepsilon_y$, $\varepsilon_u = 100\varepsilon_y$, f_e = proportional limit strength, f_y = yield strength, f_u = ultimate strength, and E_s = elastic modulus of steel.

The stress-strain relation model of concrete adopted the constitutive relation proposed by Han et al. [15], as indicated in Figure 1(b). The confinement factor ξ [14] was used to display the confinement between the steel tube and the core concrete. When $\xi \geq \xi_0$, the stress-strain curve has no descent segment. As for concrete-filled circular steel tubes, $\xi_0 = 1.12$. The damage plastic model defined in ABAQUS was used to simulate the three-way force relationship of concrete in the CFCST columns. According to previous studies [16, 17], key material parameters are determined as follows: dilation angle $\psi = 30^\circ$, flow potential offset ε (θ, f_i) = 0.1, $\sigma_{b0}/\sigma_{c0} = 1.16$, $K_c = 2/3$, and coefficient of viscosity $V_p = 0.0005$.

3. Comparison and Validation of Different Modeling Methods

In the work of Wang et al. [4], experimental research was carried out on CFCST frames under constant axial force and horizontal load. Frames CF-11 and CF-12 were selected as the simulation objects, and the fiber model based on PERFORM3D and the solid finite element model based on ABAQUS software were used, respectively, to compare two different modeling methods. Two cases were considered in the solid element model method: the first one considered the bond-slip between the outer steel tube and the inner concrete, while the other did not.

H-$150 \times 70 \times 3.44 \times 3.44\,\text{mm}^4$ and Ø$140 \times 2.0\,\text{mm}^4$ were used to fabricate the beams and columns of CF-11 and CF-12, respectively. Beams were 2.5 m in length, and columns were 1.45 m in height. The axial compression ratios of CF-11 and CF-12 were 0.07 and 0.3, respectively. The elastic

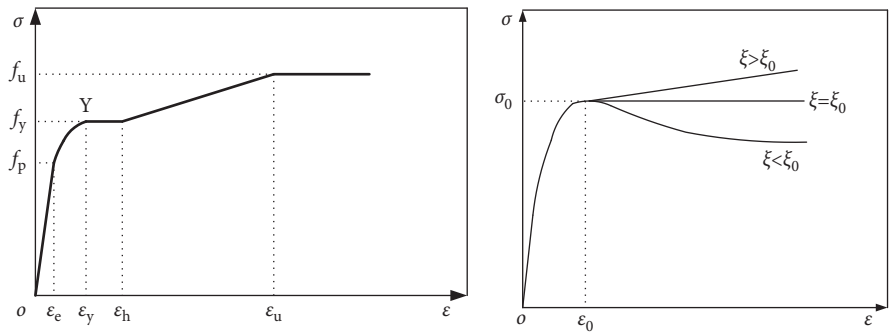

Figure 1: Stress-strain relation model. (a) Steel. (b) Concrete.

modulus E_c of concrete-filled in the steel tubular was 33800 MPa, and the compressive strength of cube f_{cu} was 52.3 MPa. Table 1 shows the mechanical properties of steel materials.

Section fiber division of the steel beam and the CFCST column is shown in Figure 2. The solid finite element model of the test frame established by ABAQUS is shown in Figure 3.

Figure 4 compares the simulation and test results. The results of the analysis are similar to the test results. Overall, in the upward part of curves, the curve simulated by the solid model (without slip) is the closest to the test curve, the curve simulated by the solid model (with slip) is slightly lower than the test curve, and the curve simulated by the fiber model method is slightly higher than the test curve. The calculated maximum load-carrying capacity is less than the test value. The two curves of the nonslip model and the slip model differ slightly only in the upward part. The calculated value of the nonslip model is slightly larger. There is little difference between the two curves in the descending phase.

Figure 5 shows the Mises stress nephogram obtained based on the slip and nonslip solid model methods, respectively. The figure shows whether the slip is considered to have little effect on the distribution of Mises stress nephogram.

From the above analysis, it can be seen that the bond-slip between the outer steel tube and the inner core concrete has no great influence on the overall response or local response of the structure. This also partly explains the rationality of the assumption of strain compatibility between steel tube and core concrete in the fiber model. In addition, although the solid element modeling method has a high degree of refinement, the modeling process is complicated, the calculation amount is large, and the time is spent, so it is not suitable for the analysis of the overall structure. Thus, the fiber modeling method is used to analyze the influence parameters of CFST frame structures.

4. Analysis of the Influence Factors of Failure Mode

The failure modes of frame structures under horizontal earthquake include beam hinge failure mode, column hinge failure mode, and mixed failure mode. The column hinge failure mode is a local failure mechanism and has the worst deformability and seismic performance. The beam hinge failure mode is an overall failure mechanism and has the best deformation and seismic performance. The mixed failure mode is intermediate. In the antiseismic design, the beam hinge failure mode or the mixed failure mode is expected to be used when the frame structure is damaged, and it is an effective measure to ensure that the frame structure can realize the weak beam-strong column. The column-to-beam flexural capacity ratio $\eta_{c,}$ beam-to-column stiffness ratio β (beamline stiffness/column line stiffness), and axial compression ratio n (design value of axial force N/ axial compression capacity N_{u0}) are the main factors behind the deformation, mechanical behavior, and failure mode of frame structures.

4.1. Column-to-Beam Flexural Capacity Ratio. The flexural capacity ratio of column to beam is the most important factor behind the failure mode of the frame structure. The CFST frame column is an eccentrically loaded component, and its flexural capacity is related to the axial force. For the sake of comparison, the column-to-beam flexural capacity ratio η_c was defined as the ratio of the nominal flexural capacity M_{u0} [18] of the CFCST column to the flexural capacity M_{ub} of the steel beam, as shown in the following equation:

$$\eta_c = \frac{M_{u0}}{M_{ub}}. \tag{1}$$

Sixteen steel beam-CFCST column plane frames were designed, including four frames of three stories, five stories, eight stories, and ten stories each. The height of the bottom story of the frame was 3.6 m, and the height of the rest was 3.0 m. The seismic fortification intensity of the site where the structure was located was 8 degrees (0.20 g), the design earthquake group was the second group, and the site classification was category II. The steel beams were all made of H-shaped beam, and the material was Q235-B. The beam section was not changed for the 4 models with the same number of stories. The steel beam of the 3-story and 5-story frame structure was $H450 \times 200 \times 9 \times 14$. The steel beam of the 8-story and 10-story frame structure was

Table 1: Mechanical properties of steel materials.

Type	Thickness (mm)	f_y (MPa)	f_u (MPa)	E_s (N/mm^2)	Poisson's ratio μ_s
Circular steel tube	2.0	327.7	397.9	2.063×10^5	0.266
Steel beam	3.44	303	440.9	2.061×10^5	0.262

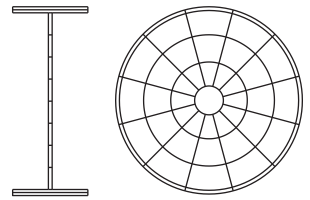

Figure 2: Fiber model of sections. (a) Beam. (b) CFCST column.

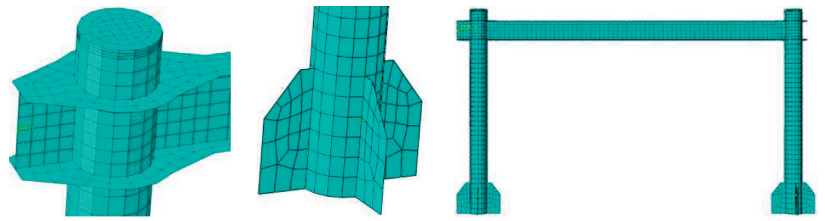

Figure 3: Solid finite element model. (a) Joint. (b) Column foot. (c) Frame.

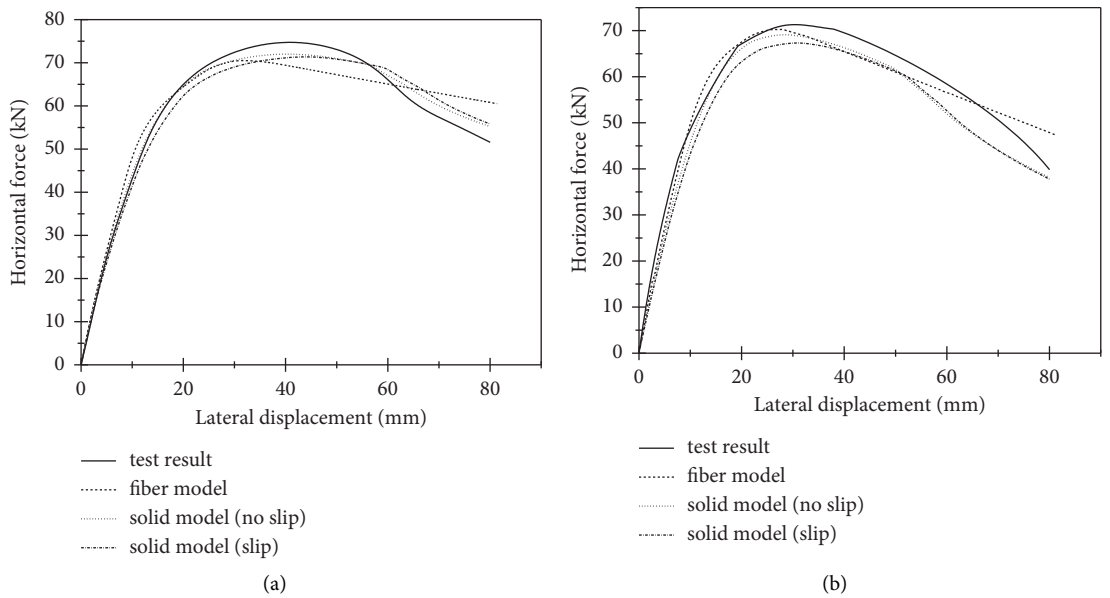

Figure 4: Comparison of calculated result with the test result. (a) CF-11. (b) CF-12.

H500 × 200 × 10 × 16. η_c values were 0.8, 1.0, 1.2, 1.6, and 2.0, and it could be realized by changing the section size of the column, the thickness of the steel pipe wall, and the material strength. For the frame with the same number of stories, the axial compression ratio and linear stiffness ratio remained unchanged. Table 2 shows the information of the frames. All frames meet the strength and deformation verification and examination requirements under many earthquakes.

The lateral load in the first mode distribution [19] was used to carry out pushover analysis on the frame structures.

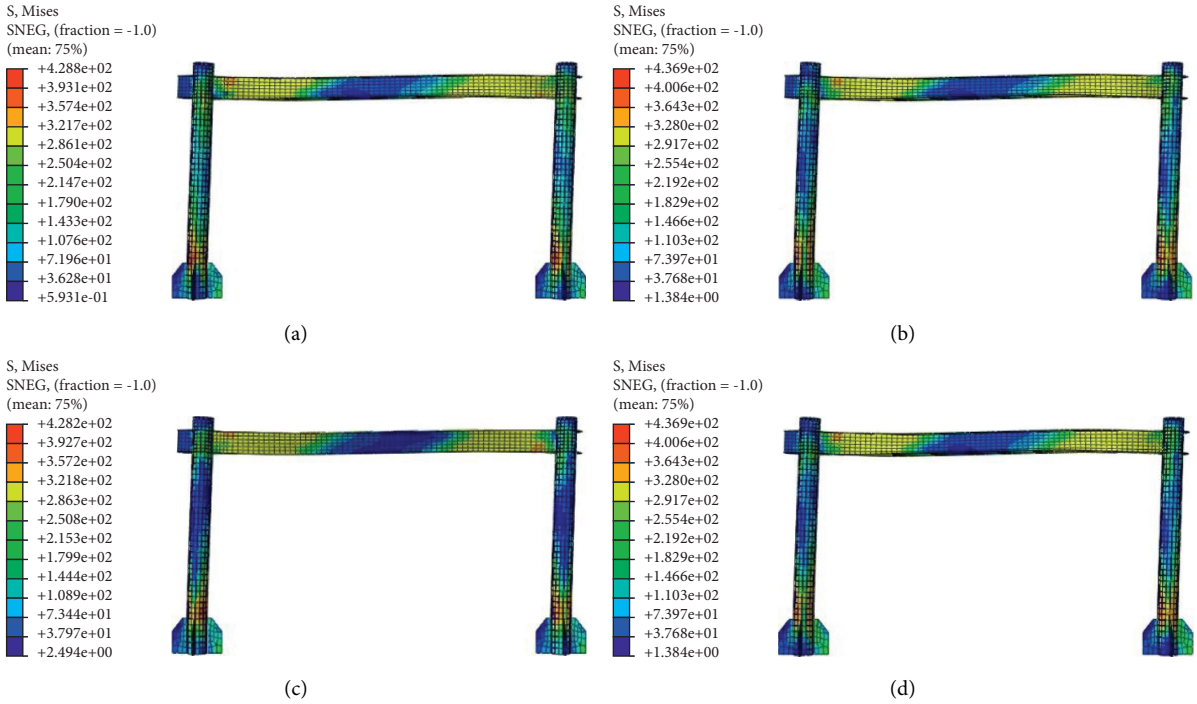

Figure 5: Mises stress nephogram. (a) CF11 (slip). (b) CF11 (no slip). (c) CF12 (slip). (d) CF12 (no slip).

Table 2: Information of frames.

η_c	3 stories and 5 stories				8 stories and 10 stories			
	Column section (mm)	Concrete	Steel	Beam span l (m)	Column section (mm)	Concrete	Steel	Beam span l (m)
1.0	450 × 6	C30	Q235	9.3	450 × 8	C35	Q235	9.1
1.2	450 × 8	C35	Q235	8.1	460 × 10	C40	Q235	7.5
1.6	470 × 10	C40	Q235	6.2	500 × 8	C40	Q345	6.1
2.0	500 × 8	C40	Q345	5.4	500 × 12	C40	Q345	5.2

Figure 6 shows the capability curves of base shear V and top drift Δ. As can be seen from the figures, as η_c gradually increases, the overall lateral stiffness, bearing capacity, and deformation capacity of the frames all increase. When η_c is less than 1.6, the deformation behavior and ductility of the structure are poor. When η_c is greater than or equal to 1.6, the structure shows good deformation behavior and ductility.

Table 3 shows the failure modes of 16 structures. When η_c is less than 1.6, the failure modes are column hinge failure ones. When η_c is equal to 1.6, the failure modes are mixed failure ones. When η_c is equal to 2.0, the failure modes are beam hinge failure modes.

Through the statistical analysis on the whole process of structural damage, it can be observed that when η_c is less than 1.6, a plastic hinge first appears at the bottom of the column on the first floor. As the lateral load increases, plastic hinges appear at the upper and lower ends of the central column in the second and third stories. Then plastic hinges continue to appear at some beam ends and column ends. The failure mode of the frame structure comes from the failure of the column hinge, and hinges in the beam are not fully developed. When η_c is equal to 1.6, the plastic hinge first appears at the end of the beam on the second floor. After the right end of the second and third floor beams yield, the plastic hinge just appears at the bottom of the column on the first floor. When the beam hinges have been developed to a certain extent, the upper column hinge is just formed. The failure mode of the frame structure is a mixed failure one. When η_c is equal to 2.0, the plastic hinge first appears at the end of the beam. When more than half of the right end of the beam yield, the plastic hinge appears at the bottom of the middle column on the first floor. As the beam hinges further develop, plastic hinges appear in the two ends of most of the beams and reach the limit, plastic hinges just appear at the top of individual columns, and the structure reaches the ultimate bearing capacity. The damage process is a typical beam hinge failure mode. The frame structure shows good ductility and seismic performance.

Take 8-story frame structures as examples. Figure 7 shows three different states in the development process of plastic hinges. The three states refer to the occurrence of the plastic hinge, the top drift up to 200 mm, and the limit state.

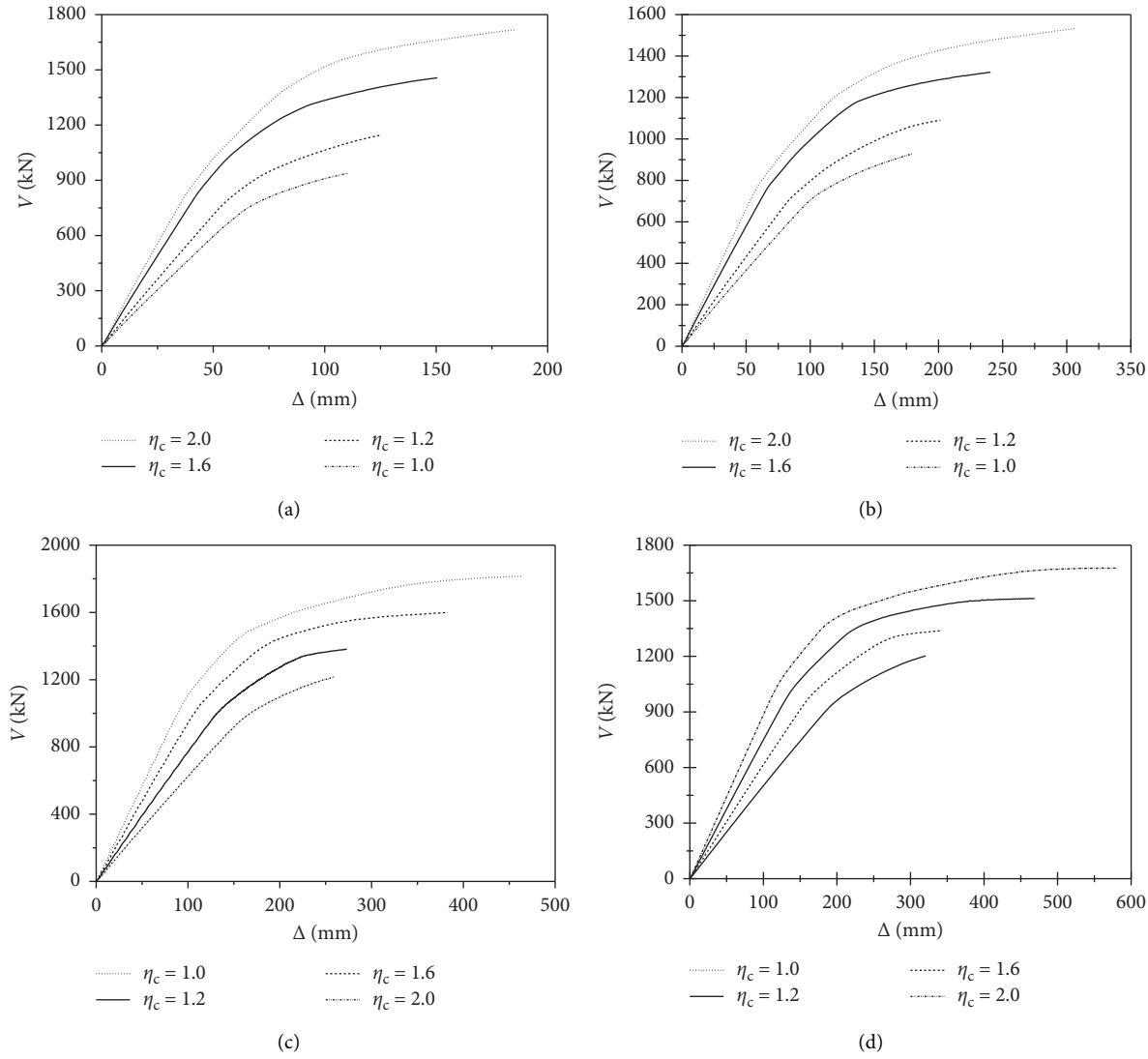

Figure 6: Capacity curves of structures with different η_c. (a) 3 stories. (b) 5 stories. (c) 8 stories. (d) 10 stories.

Table 3: Failure mode.

η_c	3 stories	5 stories	8 stories	10 stories
1.0	Column hinge failure mode	Column hinge failure mode	Column hinge failure mode	Column hinge failure mode
1.2	Column hinge failure mode	Column hinge failure mode	Column hinge failure mode	Column hinge failure mode
1.6	Mixed failure mode	Mixed failure mode	Mixed failure mode	Mixed failure mode
2.0	Beam hinge failure mode	Beam hinge failure mode	Beam hinge failure mode	Beam hinge failure mode

○ means that the plastic hinge has just entered the yield state, ⊗ indicates that the curvature of the plastic hinge is 4 times the yield curvature. ● represents that the curvature of the plastic hinge is 6 times the yield curvature. ◆ indicates that the plastic hinges reach the limit.

From the above analysis, with the increase of the column-to-beam flexural capacity ratio η_c, the initial axial compression ratio and the elastic line stiffness ratio of the beam to column remain unchanged, and the failure mode of the structure gradually changes from the column hinge failure mode to the mixed failure mode and finally to the beam hinge failure mode no matter how much the structural stories are. When η_c is less than 1.6, column plastic hinges first appear, the plastic hinge on the beam is not fully developed, the energy dissipation capacity is poor, the local failure mechanism is easy to form, and the structure shows the poor overall deformation behavior. For the purpose of ensuring that the structure can have better seismic performance under rare earthquakes or unprecedented super earthquakes, it is suggested that the column-to-beam flexural capacity ratio η_c of steel beam-CFCST column frame be greater than or equal to 1.6.

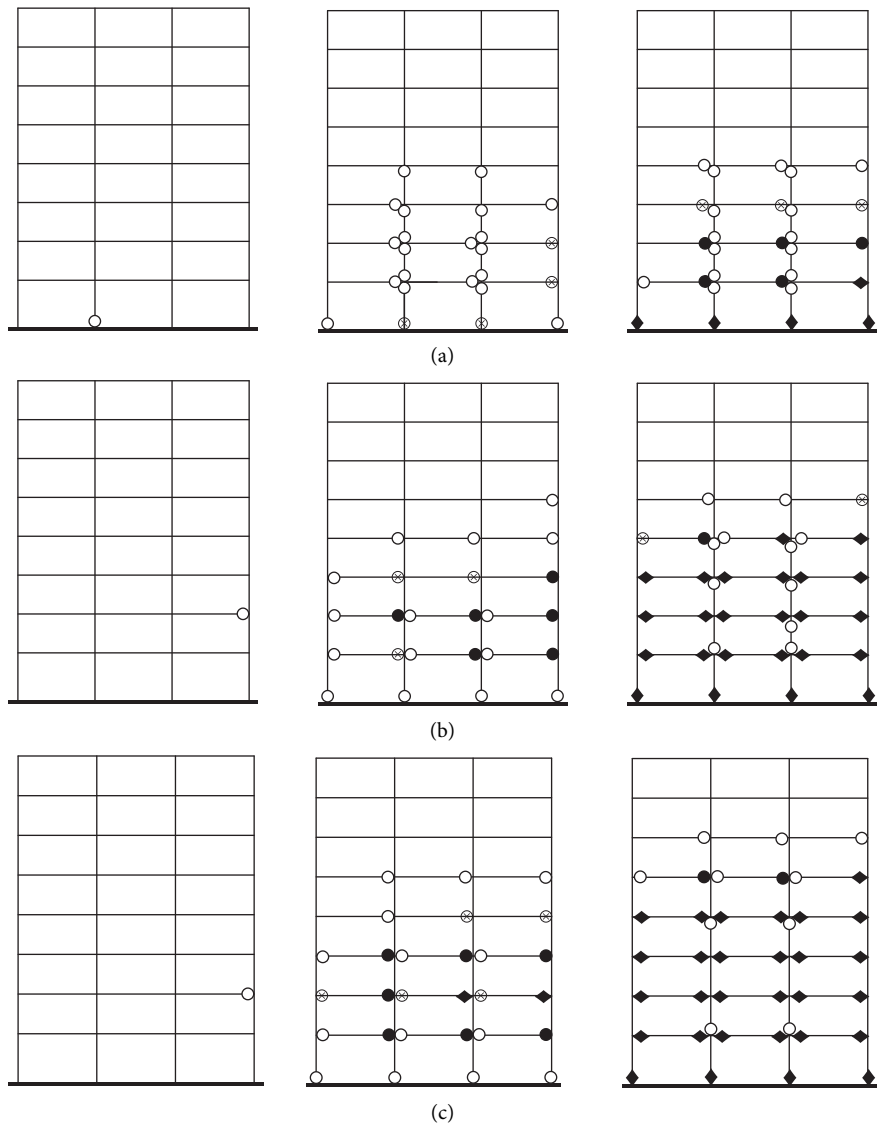

Figure 7: Plastic hinge development process for different failure mode. (a) Column hinge failure mode ($\eta_c = 1.0$). (b) Mixed failure mode ($\eta_c = 1.6$). (c) Beam hinge failure mode ($\eta_c = 2.0$).

4.2. Beam-to-Column Line Stiffness Ratio. On the basis of the 5-story and 8-story frame ($\eta_c = 2.0$) structures in Section 4.1, the beam-to-column stiffness ratio β is changed by adjusting the beam span l and the story height, while the axial compression ratio n remains changed. Eight frame structures were designed. Please check Table 4 for structural model information. All the structures meet the requirements for seismic design.

Figure 8 shows the relationship curves of base shear force V and top drift Δ obtained by the pushover analysis. For frames F52~F54 and F81~F84, when n, η_c, and the story height remain unchanged, the constraint effect of the frame beam on the frame column decreases. As β decreases and the beam span l increases, the overall lateral stiffness and bearing capacity of the frame decrease slightly, but the influence on the overall deformation capacity of the structure is not obvious. Compared with model F52, the story height of model F51 increases, the lateral stiffness of the column decreases, and the overall bearing capacity of the structure decreases greatly, but the deformation capacity of the structure has been improved to a certain extent.

The damage process of 8 structures was analyzed. With the gradual increase of the beam-to-column stiffness ratio β, the yield sequence of the structural members did not change obviously, and the plastic hinge first appeared at the end of beams. After a plastic hinge appeared at most of the beam ends, plastic hinges appeared at the bottom of the column, forming a beam hinge failure mode. Then, with the development of deformation, after the plastic hinge at both ends of the beam reached the limit state, the plastic hinge at the bottom of the column reached the limit, too. When the frame structures reached the limit, the plastic hinges at the top of the column appeared or did not appear in a few intermediate stories. The structural failure process was basically similar to Figure 7(c) and was not shown.

Table 4: Information of structural models with different β.

Frame	5 stories					Frame	8 stories				
	Story height (m)		β		l (m)		Story height (m)		β		l (m)
	1	2~5	1	2~5			1	2~5	1	2~5	
F51	4.2	3.6.	0.311	0.267	5.4	F81	3.6	3.0	0.416	0.347	4.2
F52	3.6	3.0	0.265	0.221	5.4	F82	3.6	3.0	0.339	0.282	5.2
F53	3.6	3.0	0.229	0.190	6.3	F83	3.6	3.0	0.243	0.202	7.2
F54	3.6	3.0	0.200	0.167	7.2	F84	3.6	3.0	0.208	0.173	8.4

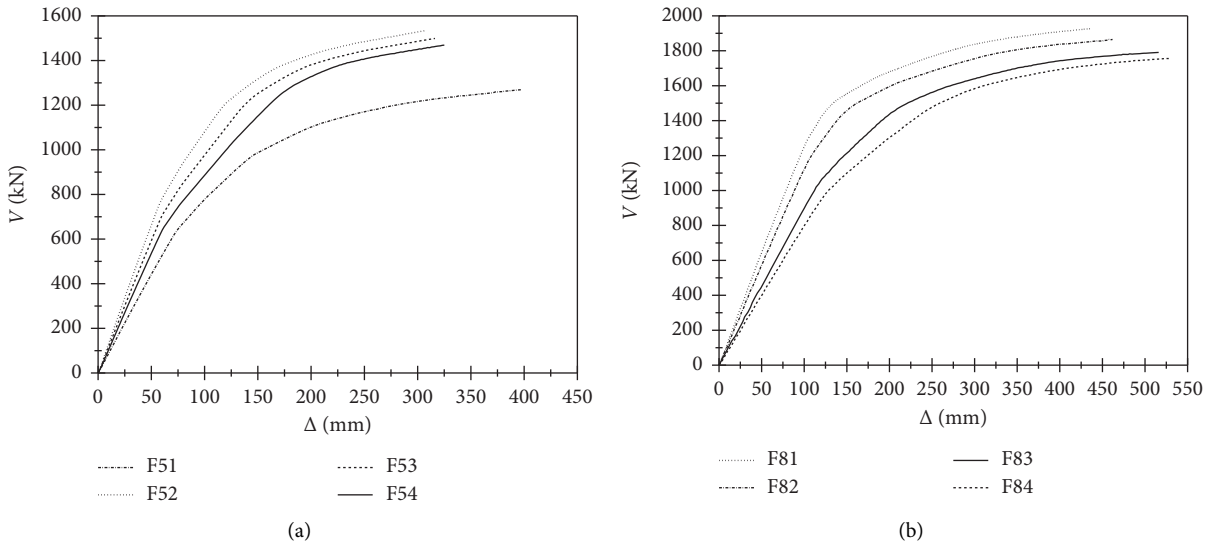

Figure 8: Capacity curves of structures with different β. (a) 5 stories. (b) 8 stories.

4.3. Applicability Analysis on Different Axial Compression Ratios. According to the flexural bearing capacity and axial compression bearing capacity formula of the CFCST column in CECS 230:2008 [18], the relevant equations of CFCST flexural components under the action of axial force N and flexural capacity M could be derived.

$$\begin{cases} \dfrac{N}{N_{u0}} + \dfrac{0.444M}{M_{u0}} = 1, & \left(\dfrac{N}{N_{u0}} \geq 0.258\right), \\ M = \dfrac{5}{3}M_{u0}, & \left(\dfrac{N}{N_{u0}} < 0.258\right), \end{cases} \tag{2}$$

where N_{u0} means axial compression bearing capacity and M_{u0} is nominal flexural capacity [18].

Figure 9 presents the M-N relative curves of the CFCST column. The x-coordinate is M/M_{u0}, and the y-coordinate is n (N/N_{u0}). When n is equal to 0.556, M is equal to M_{u0}. When n is equal to 0.645, M is equal to $0.8M_{u0}$. When n is less than or equal to 0.556, $M \geq M_{u0}$, $\eta_c \geq 2.0$, and the failure process of frames is from the beams to the columns. When $0.556 < n \leq 0.645$, $1.6 \leq \eta_c \leq 2.0$ and the failure process of frames is all about mixed failure modes. Thus, when n is less than or equal to 0.645, η_c is greater than equal to 1.6, it can be ensured that the failure mode of the frame structure is beam hinge mode or mixed failure mode, and the column hinge failure mode will not occur.

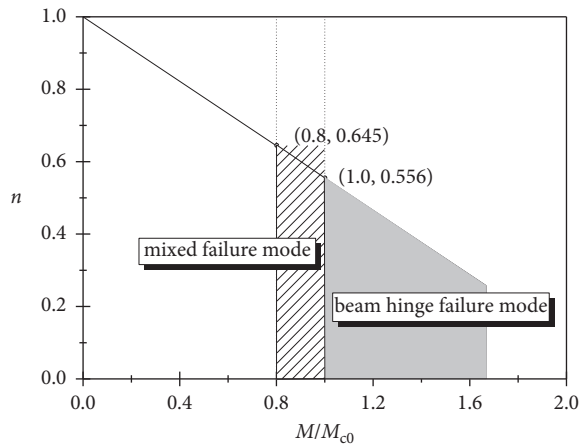

Figure 9: M-N interactive curves.

In order to further verify the above conclusions, the study designed eight frame structures based on frame F82. The axial compression ratio of the column varied between 0.2 and 1.0 by changing the upper load of the beam. Figure 10 shows the structural capability curves obtained based on pushover analysis. The axial compression ratio n gradually increases from top to bottom. As shown in the figure, as

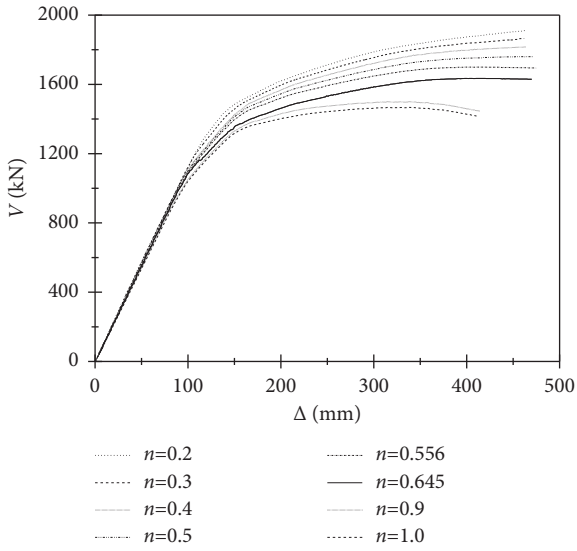

Figure 10: Capacity curves of structures with different n.

the axial compression ratio n increases, the bearing capacity of the frame structure decreases gradually, but the change of axial compression ratio n can hardly affect the lateral stiffness in the elastic stage. When n is less than or equal to 0.645, the deformation capacity and ductility of the frame structures are not affected even though the axial compression ratio n increases. However, under a high axial compression ratio, the bearing capacity is obviously reduced, and the deformation capacity of the structure is poor.

The results of failure modes from finite element modeling analysis are consistent with the results of the above theoretical analysis. When n ranges from (0.645, 1], the column hinge failure mode occurs. When n is in (0.556, 0.645], the mix failure mode occurs. When n is among (0, 0.556], the beam hinge failure mode occurs. The final failure modes of different axial compression ratio intervals are different, and the three failure modes are similar to Figure 7.

In conclusion, the flexural capacity ratio of column to beam controls the possible failure state of the frame structure at the bearing capacity. With the same column-to-beam flexural capacity ratio η_c, the normal design of beam-to-column stiffness ratio β can hardly affect the failure mode of the structure, but when the story height increases and the column linear stiffness decreases, the structural bearing capacity decreases and the deformation capacity improves. This is consistent with the concept of matching stiffness and ductility in seismic conceptual design. When the column-to-beam flexural capacity ratio η_c remains unchanged and the axial compression ratio n is less than or equal to 0.654, the change of axial compression ratio can hardly affect the failure mode of the structure. However, if the axial compression ratio is too large, the failure mode tends to be the column failure mode, and the structure is poor in seismic performance and is prone to collapse during the earthquake, so it should be avoided as much as possible in actual engineering. Therefore, the axial compression ratio of CFST frame columns should be limited under different seismic levels and seismic grades.

5. Conclusions

The fiber model method and solid finite element method are adopted to simulate the existing test model of steel beam-CFCST column frames. The advantages and disadvantages of the two modeling methods are compared, and the applicability of the two modeling methods is verified. According to the results, whether the slip between the outer steel tube and inner concrete has been taken into account in the structural analysis has little influence on the calculation results. The fiber model method can be used to analyze the elastic and elastoplastic deformation of CFCST structures.

The factors affecting the failure mode of steel beam-CFCST frame are analyzed. The influence of the column-to-bean flexural capacity ratio, beam-column line stiffness ratio, and axial compression ratio on the failure mode are studied. The suggestions are as follows: in the design, the column-to-bean flexural capacity ratio is greater than or equal to 1.6 and the axial compression ratio is less than or equal to 0.654 so as to achieve strong column-weak beam for steel beam-CFCST column frame structures.

Data Availability

The data used to support the findings of this study are included within the article.

Conflicts of Interest

The authors declare that there are no conflicts of interest regarding the publication of this paper.

Acknowledgments

This research project was supported by the Key Scientific Research Project of Henan Province (Grant no. 16B560005).

References

[1] Z. X. Zuo, M. S. Gong, J. Sun, and H. Zhang, "Seismic performance of RC frames with different column-to-beam flexural strength ratios under the excitation of pulse-like and non-pulse-like ground motion," *Bulletin of Earthquake Engineering*, vol. 23, no. 6, pp. 1–21, 2021.

[2] L. Luo, B. H. Cheng, and H. Lv, "Finite element analysis for quasi dynamic behavior of concrete filled circular steel tubular composite space frame," *Earthquake Engineering and Engineering Dynamics*, vol. 41, no. 3, pp. 124–135, 2021.

[3] L. P. Ye, Q. L. Ma, and Z. W. Miao, "Study on weak beam-strong column design method of RC frame structures," *Engineering Mechanics*, vol. 27, no. 12, pp. 102–113, 2010.

[4] W. D. Wang, L. H. Han, and Z. Tao, "Experimental research on seismic behavior of concrete filled CHS and SHS columns and steel beam planar frames," *Journal of Building Structures*, vol. 27, no. 3, pp. 48–58, 2006.

[5] W. D. Wang and L. H. Han, "Nonlinear finite element analysis on mechanical performance of concrete filled steel tubular frame structure," *Journal of Building Structures*, vol. 29, no. 6, pp. 75–83, 2008.

[6] X. F. Ding, Z. C. Pan, and L. Luo, "Preliminary investigation of the ultimate seismic resistance of steel-concrete composite

frame structure. Steel Construction," 2021, https://kns.cnki.net/kcms/detail/10.1609.TF.20210115.1631.006.html, Chinese.

[7] X. Q. Liu, C. X. Xu, and L. Li, "Application of OpenSees on calculating lateral force-displacement hysteretic curves ofconcrete-filled steel tubular frame with unequal spans," *World Earthquake Engineering*, vol. 37, no. 3, pp. 111–117, 2021.

[8] Y. B. Liu, F. Chen, and J. B. Liu, "Research on weak beam-strong column design method of steel-concrete composite frame structures," *Journal of Sichuan University (Engineering Science Edition)*, vol. 44, no. 4, pp. 20–25, 2012.

[9] C. Fang, F. Zhou, Z. Wu, and F. C. Wang, "Concrete-filled elliptical hollow section beam-columns under seismic loading," *Journal of Structural Engineering*, vol. 146, no. 8, Article ID 04020144, 2020.

[10] A. Fam, F. S. Qie, and S. Rizkalla, "Concrete-filled steel tubes subjected to axial compression and lateral cyclic loads," *Journal of Structural Engineering*, vol. 130, no. 4, pp. 631–640, 2004.

[11] Z. Tao, U. Katwal, B. Uy, and W. D. Wang, "Simplified nonlinear simulation of rectangular concrete-filled steel tubular columns," *Journal of Structural Engineering*, vol. 147, no. 6, Article ID 04021061, 2021.

[12] Components and Structures, *Perform-3D Version 5*, Components and Structures Inc., Berkeley, CA, USA, 2011.

[13] L. H. Han, W. D. Wang, and X. L. Zhao, "Behavior of steel beam to concrete-filled SHS column frames: finite element model and verifications," *Engineering Structures*, vol. 30, no. 6, pp. 1647–1658, 2008.

[14] L. H. Han, X. L. Zhao, and Z. Tao, "Tests and mechanics model for concrete-filled SHS stub columns, columns and beam-columns," *Steel and Composite Structures*, vol. 1, no. 1, pp. 51–74, 2001.

[15] L. H. Han, G. H. Yao, and X. L. Zhao, "Tests and calculations of hollow structural steel (HSS) stub columns filled with self-consolidating concrete (SCC)," *Journal of Constructional Steel Research*, vol. 61, no. 9, pp. 1241–1269, 2005.

[16] Z. Tao, Z. B. Wang, and Q. Yu, "Finite element modelling of concrete-filled steel stub columns under axial compression," *Journal of Constructional Steel Research*, vol. 89, pp. 121–131, 2013.

[17] Y. O. Tu, Y. F. Shen, and P. Li, "Behaviour of multi-cell composite T-shaped concrete-filled steel tubular columns under axial compression," *Thin-Walled Structures*, vol. 85, pp. 57–70, 2014.

[18] China Planning Press, *Specification for Design of Steel-concrete Mixed Structure of Tall Buildings (CECS230:2008)*, China Planning Press, Beijing, China, 2008.

[19] J. B. Liu, Y. B. Liu, and Q. S. Yan, "Performance-based seismic fragility analysis of CFST frames," *China Civil Engineering Journal*, vol. 43, no. 2, pp. 39–47, 2010.